Role of the Hoggar massif in the West African monsoon onset

Philippe Drobinski,[1] Benjamin Sultan,[2] and Serge Janicot[2]

Received 9 June 2004; revised 2 September 2004; accepted 24 November 2004; published 13 January 2005.

[1] It has been observed that the West African monsoon onset is concomitant with the enhancement of the Saharan heat low. We show through a combined diagnostic and linear modeling study a possible interaction between northern Africa orography and the deepening of the Saharan heat low at the time of the monsoon onset. The amplification of an anticyclonic circulation above and north of the Hoggar massif leads to an increase and a southeasterly-northeasterly rotation of the wind ahead of the Hoggar which contribute to an increased leeward-trough effect enhancing the Saharan heat low. The Atlas does not play any role during the monsoon onset but contributes to the mean climatological location of the Saharan heat low.
Citation: Drobinski, P., B. Sultan, and S. Janicot (2005), Role of the Hoggar massif in the West African monsoon onset, *Geophys. Res. Lett.*, *32*, L01705, doi:10.1029/2004GL020710.

1. Introduction

[2] The onset of the summer monsoon over West Africa is linked to an abrupt latitudinal shift of the Inter-Tropical Convergence Zone (ITCZ) from a quasi-stationary location at 5°N in May–June to another quasi-stationary location at 10°N in July–August [*Le Barbé et al.*, 2002; *Sultan and Janicot*, 2003]. In the last 35 years, the mean date for the onset occurrence has been 24 June and its standard deviation 8 days. This abrupt shift occurs mostly between 10°W and 5°E where a meridional land-sea contrast exists; it is characterized by a temporary rainfall and convection decrease over West Africa. *Sultan and Janicot* [2003] suggested this abrupt ITCZ shift is associated with the low and mid levels atmospheric dynamics of the Saharan heat low located between 15°N and 20°N. The latitude gap between ITCZ and the heat low is due to a similar gap between the maximum in the meridional profile of moist and dry static energy, respectively. The heat low meridional circulation intensity is the highest at the beginning of the monsoon onset, leading to both an increase in convective inhibition in the ITCZ through intrusion of dry and subsiding air from the north, and an increase in potential instability through a greater inland moisture advection and a higher monsoon depth induced by a stronger cyclonic circulation in the low-levels. During the monsoon onset, once the rainfall minimum occurred due to the convective inhibition, the accumulated potential instability breaks the convective inhibition, the inertial instability of the monsoon circulation is released and the associated regional scale circulation increases, leading to the abrupt shift of the ITCZ. Then the ITCZ moves north to 10°N, where thermodynamical conditions are favorable. *Sultan and Janicot* [2003] suggested the amplification of the heat low dynamics, associated with the abrupt monsoon onset, could be due to an interaction with the northern orography of the Atlas-Hoggar mountains. Subsidence over and north of this orography, due to the Northern Hemisphere branches of the heat low and the northern Hadley-type cell, could contribute to enhance the high geopotentials north of these mountains and the associated northeasterly winds, leading to the development of a leeward trough south of these mountains.

[3] The aim of this paper is to investigate this orography-induced forcing of the heat low dynamics during the West African monsoon onset by using results of the composite approach described by *Sultan and Janicot* [2003] applied to the NCEP-NCAR atmospheric reanalyses. Results will be compared with simulations of a linear model describing the atmospheric circulation anomalies in response to orography. An analytical linear model is developed here to calculate the surface pressure perturbation produced by orographic internal gravity waves on the f-plane generated in a flow with constant Brunt–Väisälä frequency N over an isolated mountain of height h_0. The model is linear [*Koffi et al.*, 1998], and hence valid for a dimensionless height $\hat{h} = Nh_0/|\mathbf{U}| \ll 1$, where $\mathbf{U} = (U, V)$ is the wind.

2. The Composite Approach

[4] The National Centers for Environmental Prediction (NCEP) and the National Center for Atmospheric Research (NCAR) have completed a reanalysis project with a current version of the Medium Range Forecast model [*Kalnay et al.*, 1996]. It consists of a reanalysis of the global observational network of meteorological variables with a "frozen" state-of-the-art analysis and forecast system at a triangular spectral truncation of T62 to perform data assimilation throughout the period 1948 to present. Data are reported on a 2.5° × 2.5° grid every 6 hours on 17 pressure levels from 1000 hPa to 10 hPa, which are good resolutions for studying synoptic weather systems. *Diedhiou et al.* [1999] showed that this dataset provides accurate atmospheric fields after 1968.

[5] *Sultan and Janicot* [2000, 2003] applied a quasi-objective method to define a date of the monsoon onset by using daily gridded rainfall data from 1968–1990, and then used these dates, called t_0, as a respective reference date for each year to define the composite mean atmospheric patterns which might control the abrupt shift of the ITCZ around t_0. Figure 1 shows such a result for the composite mean Sea Level Pressure (SLP) and 1000 hPa wind fields at t_0 minus 5 days, t_0 plus 5 days, and the

[1]Service d'Aeronomie, Institut Pierre-Simon Laplace, Ecole Polytechnique, France.
[2]Laboratoire d'Océanographie Dynamique et de Climatologie (LODYC), Institut Pierre-Simon Laplace, Université Pierre et Marie Curie, France.

0094-8276/05/2004GL020710

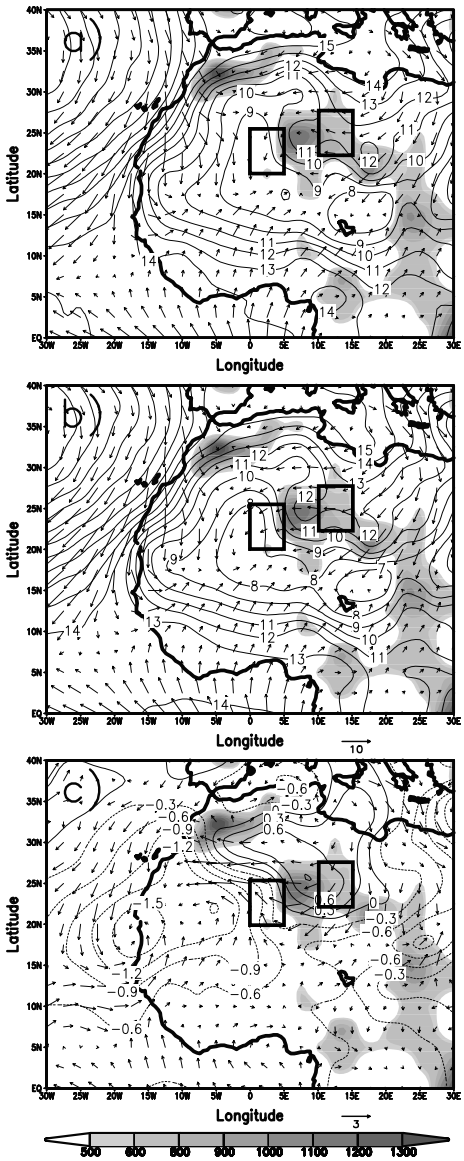

Figure 1. (a) Composite mean sea level pressure and 1000 hPa wind field (vector scale (m s^{-1}) is displayed below) at $t_0 - 5$ averaged over the period 1968–1990 by using as the reference date t_0 the ITCZ shift date for each year. Mean sea level pressure is expressed in hPa where the 1000 hPa value is subtracted. Shaded areas depict the orography of northern Africa (m). (b) Same as (a) but for $t_0 + 5$. (c) Difference between (b) and (a). Boxes used for the time series of Figure 2 are plotted.

difference between $t_0 + 5$ and $t_0 - 5$. Shaded areas depict the orography of northern Africa with the Atlas mountains centered at 5°W–32.5°N, the Hoggar mountains at 7.5°E–25°N, the Tibesti mountains at 17.5°E–20°N, and the Ennedi mountains at 23°E–15°N.

[6] At $t_0 - 5$ (Figure 1a), the axis of low pressure of the Saharan heat low follows the southern border of the northern African orography in a southeast-northwest crescent-shaped, with a high pressure gradient over the mountains crest east of the Greenwich meridian. West of 0°W, a pressure gradient is also present over the Atlas mountains, mainly controlled by the Azores anticyclone over the tropical Atlantic. The lowest pressure area is located in the Bilma erg (15°E–15°N) surrounded by mountains which prevent air ventilation and allow enhanced convection inducing surface pressure low. The composite surface temperature from the reanalyses show evidence of a surface temperature maximum (33°C), 2°C warmer than outside the Bilma erg (not shown). At $t_0 + 5$ (Figure 1b), the pressure gradient over the orography east of 0°W has clearly increased due to enhancement of the high pressures in the north and intensification of the heat low in the south. In particular, the 1008 hPa isoline depicts the low deepening along 0°W and the 1007 hPa isoline the low enhancement in the Bilma erg. This evolution is shown by the difference field in Figure 1c. Aside from the orography-related dipole pressure field enhancement, we observe also a westward extension of the low pressure area over the western coast of West Africa, leading to the enhancement of westerly moist air advection from the tropical Atlantic feeding the ITCZ convection. Associated with the enhancement of the anticyclonic circulation north of the Hoggar massif, we notice that the wind direction has changed. Upstream of the Hoggar, the wind changed from easterly/southeasterly to easterly/northeasterly, leading from a pattern where the wind is tangential to the mountain crest line to a pattern where it flows in a more perpendicular way. Figure 1c shows that this change in direction is linked to the enhanced pressure pattern located upstream and above the Hoggar.

[7] Figure 2 (red lines) shows the composite time series of the 1000 hPa wind direction (thin line) and speed (bold line) averaged over the area (10°E–15°E/22.5°N–27.5°N) upstream of the Hoggar. The shift of the wind direction from 100° to 80° is clear between t_0 and $t_0 + 1$. A Mann-Whitney-Pettitt test [*Pettitt*, 1979] confirms that the monsoon onset is the most significant change point in the wind direction time series with a probability P greater than 0.99. Also, an increase of the wind speed from 3 m s^{-1} to 4 m s^{-1}

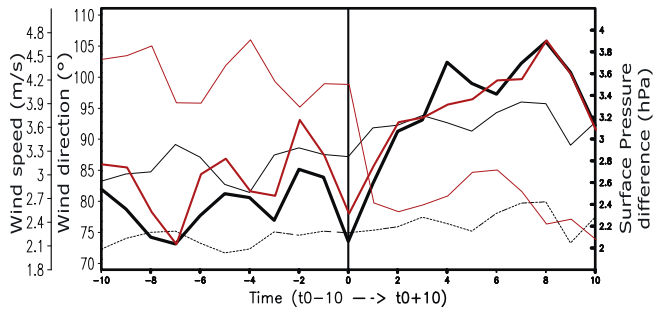

Figure 2. Red lines: Composite time series from $t_0 - 10$ to $t_0 + 10$ of the 1000 hPa wind speed (bold line) and direction (thin line) averaged over the area (10°E–15°E/22.5°N–27.5°N) upstream of the Hoggar. Black lines: Composite time series of the difference between the mean sea level pressure averaged over the area (10°E–15°E/22.5°N–27.5°N) upstream of the Hoggar and over the area (0°W–5°E/20°N–25°N) downstream of the Hoggar (bold line); these two boxes are displayed on Figure 1; dotted line: same as thick line but for the simulation due to the Atlas alone. Thin line: same as thick line but for the simulation due to the three massifs.

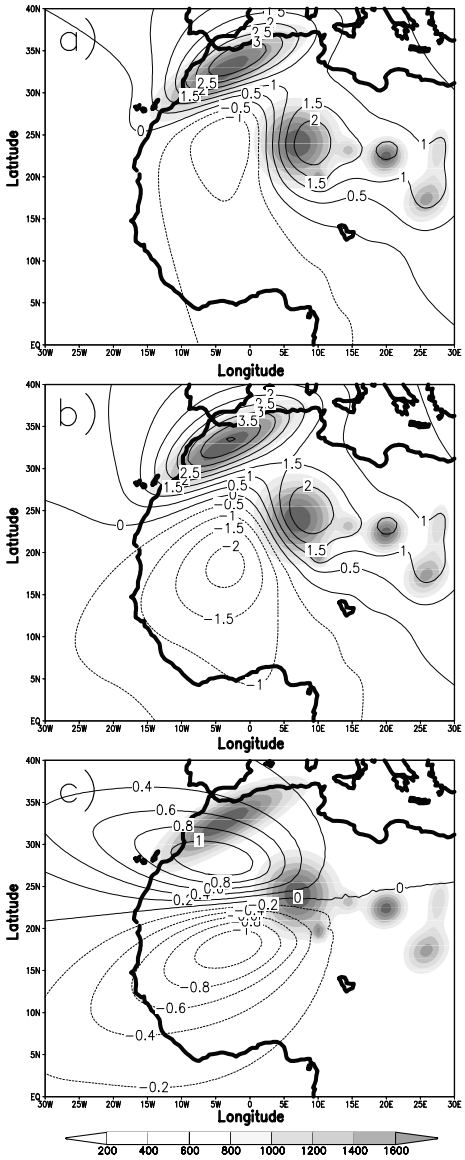

Figure 3. Surface pressure perturbation from the linear model due to the orographic effect (a) before the monsoon onset (similar to $t_0 - 5$), (b) after the monsoon onset (similar to $t_0 + 5$) and (c) the difference between (b) and (a). Shaded areas depict the idealized orography of northern Africa used in the linear model (m).

is depicted. However, no similar signal is found at t_0 upstream of the Atlas mountains and of the Ennedi, mountains (not shown): between $t_0 - 10$ and $t_0 + 10$, the 1000 hPa wind upstream of the Atlas is rather constant in direction (northwest) and no trend is evident in its strength; upstream of the Ennedi mountains, the wind speed is nearly constant with a weak variability and the wind direction is about 35° with a smooth decreasing trend from about 40° to 30°. Similar results have been obtained when considering the wind at 925 hPa (not shown). Figure 2 (bold black line) also displays the difference between the mean SLP over the area (10°E–15°E/22.5°N–27.5°N) upstream of the Hoggar (see the boxes in Figure 1), and over the area (0°W–5°E/20°N–25°N) downstream of the Hoggar. The surface pressure difference before the onset is about 2.4 hPa and sharply increases to 3.6 hPa after the onset. The Mann-Whitney-Pettitt test shows there is high probability for the monsoon onset being a change point (P = 0.99). So the presence of the Hoggar massif seems to have an impact on the monsoon onset as the upstream wind veers from the east/southeast to the east/northeast and its speed increases from 3 m s^{-1} to 4 m s^{-1}, due to the anticyclonic circulation increase above and north of the Hoggar (Figure 1c). The upstream air mass thus impinges upon the Hoggar massif almost perpendicularly to the crest line. This wind rotation and speed increase are highly correlated with the pressure gradient (correlation coefficients amounting to −0.79 and +0.92 respectively, over the period $t_0 - 15/t_0 + 20$).

3. Comparison With Linear Theory

[8] In this section, a linear theory is used to investigate the origin of the surface low deepening downstream the Hoggar massif at the monsoon onset. In absence of roughness effect, the surface pressure perturbation p'_s induced by the mountains on the incoming flow (with constant wind component U, V in the x and y directions, background mean air pressure p and density ρ) is computed from its inverse Fourier transform $\tilde{p}$ given by the linear theory [*Koffi et al.*, 1998]:

$$\tilde{p} = i\rho \frac{N^2}{m} \tilde{h} \tag{1}$$

where $N = [(g/\theta)\ (\partial\theta/\partial z)]^{1/2}$ is the Brunt-Väisälä frequency (θ is the potential temperature), $\tilde{h}$ the inverse Fourier transform of the orography $h(x, y)$ and m is the vertical wavenumber given by:

$$m^2 = \left[\frac{k^2 + l^2}{(Uk + Vl)^2 - f^2}\right] N^2 \tag{2}$$

where k and l are the wavenumbers in the x and y directions and f is the Coriolis parameter. The surface pressure, a particularly interesting variable, can be easily compared with the NCEP reanalyses. In order to limit the number of Fourier modes and investigate the perturbation of the flow over individual groups of mountain ranges (Atlas, Hoggar and Ennedi), the topography was smoothed and an analytical expression of each group of mountains was derived (see Figure 3).

[9] Similar to the study of the NCEP/NCAR composite SLP, the average upstream variables (surface pressure, wind speed and direction) were calculated over the area (10°E–15°E/22.5°N–27.5°N) (see Figure 1). The average downstream variables were calculated over the area (0°W–5°E/20°N–25°N). The inputs for the linear model, before and after the monsoon onset, are the mean wind speed and direction, the Brunt-Väisälä frequency, here assumed to be constant and equal to its climatological value of 10^{-2} s^{-1} and the Coriolis parameter, upstream the Atlas ridge, the Hoggar massif and the Ennedi mountains. A uniform stratification of the atmosphere is assumed to keep the parameter space of the problem at a reasonable level. However the vertical structure of this region is character-

Table 1. Input Variables for the Linear Model Before and After the Monsoon Onset Upstream of the Atlas Ridge (ATL), the Hoggar Massif (HOG) and the Ennedi Mountains (ENN)[a]

	f (s^{-1})	ff (m s^{-1})	dd (°)
ATL	8.3×10^{-5}	4.1/3.8	325/331
HOG	6.5×10^{-5}	3.2/4.0	102/84
ENN	3.8×10^{-5}	4.6/5.7	37/31

[a]The variable f is the Coriolis parameter, ff the wind speed, dd the wind direction. The variables before ($t_0 - 5$) and after ($t_0 + 5$) the monsoon onset are separated by a slash symbol (/).

ized by a deep planetary boundary layer (4–5 km deep corresponding to the Sahara atmospheric layer) capped by an inversion layer underneath a weaker stability layer in the mid to upper troposphere due to the subsiding branch of the Hadley cell. The stability of those three layers is different (very low, strong, moderate) and future work will be dedicated to analyse the mass pressure change due to mass change. The input values are summarized in Table 1. Typical average values of the mountain height h_0 are about 800 m for the three mountain groups. The widths a in the axis perpendicular to the upstream wind direction of the three groups of mountains are about 2000 km, 1000 km and 500 km, respectively. These values give typical dimensionless height $\hat{h} = Nh_0/|\mathbf{U}|$ and the Rossby number $|\mathbf{U}|/fa$ of 1.6–2 and 0.02–0.2, respectively. These high values of $\hat{h}$ (>1) indicate that we are pushing the small-amplitude assumption [*Smith*, 1982]. However, because of the small Rossby number, the linear theory remains valid for higher values of $\hat{h}$ [*Ólafsson and Bougeault*, 1997] and was validated with respect to empirical data during the PYREX experiment [*Ólafsson and Bougeault*, 1997; *Bénech et al.*, 1998; *Koffi et al.*, 1998].

[10] Figure 3 shows the surface pressure perturbation before and after the monsoon onset resulting from the sum of the surface pressure perturbation computed using the linear model on each group of mountains. The surface pressure pattern displays similarities with the NCEP/NCAR surface pressure field shown in Figure 1. The Atlas ridge induces a basic surface pressure low on the lee side due to the northwesterly low level flow. The surface pressure difference between the windward side and the leeward side of the Hoggar computed using the linear model is about 2.6 hPa which is in agreement with the surface pressure difference computed using the NCEP/NCAR reanalyses (see Figure 2). The absence of surface low over the Bilma erg is due to the fact that this surface pressure low is thermally induced (confirmed by a surface temperature maximum in the reanalyses). The surface pressure field from the linear model shows an increasing surface high upstream the Hoggar massif and decreasing leeward low at about 5°W and 17.5°N, which is about 5° latitude to the south with respect to the NCEP/NCAR surface low. The surface pressure difference computed using the linear model increases after the monsoon onset and is about 3.2 hPa which is in agreement with the NCEP/NCAR reanalyses (see Figure 2). Figure 3c shows the difference of the surface pressure perturbation fields between $t_0 + 5$ and $t_0 - 5$. The resulting field fairly agrees with Figure 1c except that the pressure increase downstream the Atlas and upstream the Hoggar massif is slightly shifted to the south-west. This discrepancy is caused by the fact that homogeneous wind direction is used in the linear model. Before the monsoon onset a southeasterly flow is used in the model (see Table 1) which is a correct upstream condition north and northeast of the Hoggar but is inaccurate southeast of the Hoggar where the upstream flow blows from the northeast. Figure 2 shows also the time series of the surface pressure difference between the two boxes (see Figure 1) due to the Atlas alone (dotted line), and the three massifs (thin line). The Atlas-related gradient is rather constant and can be associated with the mean climatological signal of the Saharan heat low. The contribution of the Ennedi massif is negligible (not shown). The contribution of the three massifs is similar to the observation and is closely linked to the impact of the Hoggar alone. However, looking at Figure 2, it appears that the time evolution of the pressure difference between the areas upstream and downstream the Hoggar, explained by the linear theory, agrees quite well with the composite analysis, except that the abrupt change at the onset date is not reproduced. Since the wind intensity and direction exhibit a shift at onset date, one may expect a shift for the pressure difference. The abrupt change of pressure difference in the NCEP reanalyses is thus probably due to an abrupt change in the mass field which is a point that cannot be answered in the present analysis.

4. Conclusion

[11] These results confirm a possible interaction between northern Africa orography and the deepening of the Saharan heat low at the time of the monsoon onset. The amplification of an anticyclonic circulation above and north of the Hoggar massif leads to an increase and a southeasterly-northeasterly rotation of the wind ahead of the Hoggar which contributes to an increased leeward trough effect enhancing the Saharan heat low. The Atlas does not play any role during the monsoon onset but contributes to the mean climatological location of the Saharan heat low. However linear models are practically limited to simple types of flow that is a small set of orography shapes and/or highly simplified wind profiles and stratification. Consideration of more complicated orography shapes and/or velocity and stratification profiles requires the use of approximate methods and numerical simulations.

[12] **Acknowledgment.** We are thankful to S. Chouarfi and M. Mellah for their help in analyzing the NCEP/NCAR reanalysis dataset; to Climate Diagnostics Center (NOAA, Boulder, CO) for providing the NCEP/NCAR Reanalysis dataset.

References

Bénech, B., et al. (1998), Dynamic characteristics of regional flows around the Pyrénées in view of the PYREX experiment. Part I: Analysis of the pressure and wind fields and experimental assessment of the applicability of the linear theory, *J. Appl. Meteorol.*, *37*, 32–52.

Diedhiou, A., S. Janicot, A. Viltard, P. de Felice, and H. Laurent (1999), Easterly wave regimes and associated convection over West Africa and the tropical Atlantic: Results from NCEP/NCAR and ECMWF reanalyses, *Clim. Dyn.*, *15*, 795–822.

Kalnay, E., et al. (1996), The NCEP/NCAR 40-year reanalysis project, *Bull. Am. Meteorol. Soc.*, *77*, 437–471.

Koffi, E., B. Bénech, J. Stein, and B. Terliuc (1998), Dynamic characteristics of regional flows around the Pyrénées in view of the PYREX

experiment. Part II: Solution of a linear model compared to field measurements, *J. Appl. Meteorol.*, *37*, 53–71.

Le Barbé, L., T. Lebel, and D. Tapsoba (2002), Rainfall variability in West Africa during the years 1950–90, *J. Clim.*, *15*, 187–202.

Ólafsson, H., and P. Bougeault (1997), The effect of rotation and surface friction on orographic drag, *J. Atmos. Sci.*, *54*, 193–210.

Pettitt, A. N. (1979), A non-parametric approach to the change-point problem, *Appl. Stat.*, *28*, 126–135.

Smith, R. B. (1982), Synoptic observations and theory of orographically disturbed wind and pressure, *J. Atmos. Sci.*, *39*, 60–70.

Sultan, B., and S. Janicot (2000), Abrupt shift of the ITCZ over West Africa and intra-seasonal variability, *Geophys. Res. Lett.*, *27*, 3353–3356.

Sultan, B., and S. Janicot (2003), The West African monsoon dynamics. Part II: The "preonset" and "onset" of the summer monsoon, *J. Clim.*, *16*, 3407–3427.

P. Drobinski, Service d'Aeronomie, Institut Pierre-Simon Laplace, Ecole Polytechnique, F-91128 Palaiseau cedex, France. (philippe.drobinski@aero.jussieu.fr)

S. Janicot and B. Sultan, LODYC, IPSL, Université Pierre et Marie Curie, Tour 45/55, 4eme etage, Boite 100, 4 Place Jussieu, F-75252 Paris cedex 05, France. (serge.janicot@lodyc.jussieu.fr; benjamin.sultan@lodyc.jussieu.fr)